Twenty-Seventh Symposium (International) on Combustion/The Combustion Institute, 1998/pp. 563–569

EFFECTS OF FINITE TIME RESPONSE AND SOOT DEPOSITION ON THIN FILAMENT PYROMETRY MEASUREMENTS IN TIME-VARYING DIFFUSION FLAMES

WILLIAM M. PITTS,[1] KERMIT C. SMYTH[1] AND DAVID A. EVEREST[2]

[1]*Building and Fire Research Laboratory*
National Institute of Standards and Technology
Gaithersburg, MD 20899, USA
[2]*Mechanical Engineering Department*
University of Michigan
Ann Arbor, MI 48109-2125, USA

Prior work has shown that thin filament pyrometry (TFP) is a powerful approach for making highly precise, spatially and temporally resolved line measurements of temperature in time-varying laminar diffusion flames. The technique has been previously used to map out temperature distributions as a function of phase angle for acoustically locked flickering diffusion flames with two different levels of forcing. During these measurements two small errors in the temperature measurements have been identified for certain heights and phases. The first error source is shown to be due to the limited time response of the TFP to a rapidly changing temperature field by comparing temperatures determined by TFP with line measurements using Rayleigh light scattering (RLS). The TFP measurements yield lower temperature readings when the flame front is moving at its fastest rate, but the RLS measurements show that these lower temperatures are an artifact which is attributed to the finite time response of TFP. The second source of error occurs for a limited number of cases in which soot is thermophoretically deposited on the filament and is not subsequently burned off. The soot modifies both the emissivity of the filament surface and, for large amounts of deposition, its diameter. These modifications lead to lower measured filament temperatures for low levels of soot deposition and to increasing measured temperatures as the soot builds up. Approaches are suggested for identifying the presence of these errors and minimizing their effects.

Introduction

The use of thin-filament pyrometry (TFP) for measuring flame temperatures with high spatial and temporal resolution was pioneered by Vilimpoc et al. [1]. The theory and development of the technique are discussed in several publications [2–5]. All of these investigations recorded light emission along a β-SiC fiber stretched through a flame by scanning an image of the fiber across a single photodetector. A β-SiC filament acts as a gray body, and the emission intensity can be related to the filament temperature and, hence, to the temperature of the surrounding gases. The TFP approach is subject to limitations, including the need to correct for radiative losses and the finite heat-transfer rate from the gas to the fiber. Earlier papers on the technique [1–5] should be consulted for details.

Recently, Pitts extended the TFP measurements by replacing the single detector with a cooled, two-dimensional CCD array [6]. A major advantage of this approach is that temperature data can be obtained in the presence of background luminosity from soot, but the ability to make rapid real-time measurements is lost. The approach was demonstrated by recording phase-resolved line measurements of temperature for an acoustically forced, time-varying laminar methane–air diffusion flame that had been previously investigated using a wide variety of optical techniques [7–13]. TFP measurements were possible over a 1200–2100 K range having a spatial resolution of 100 μm, a temporal resolution of $\approx$1.5 ms, and a precision on the order of 1.5 K for high flame temperatures [6]. Even though the precision was exceptionally high ($\approx$0.1% at 2000 K), the accuracy was not nearly as well defined due to uncertainties associated with radiation losses. Since the detailed information required for radiation corrections was not available, an approach was utilized in which the strongest emission from the filament in a steady laminar flame was assigned a value of 2000 K based on thermocouple measurements [14], and temperatures for other locations were calculated from the observed intensities relative to this value. The results were referred to as measured filament temperatures (MFTs) to emphasize the fact that they were uncorrected for radiative heat transfer. Even though the resulting temperatures were approximate, radial profiles recorded 7 mm above

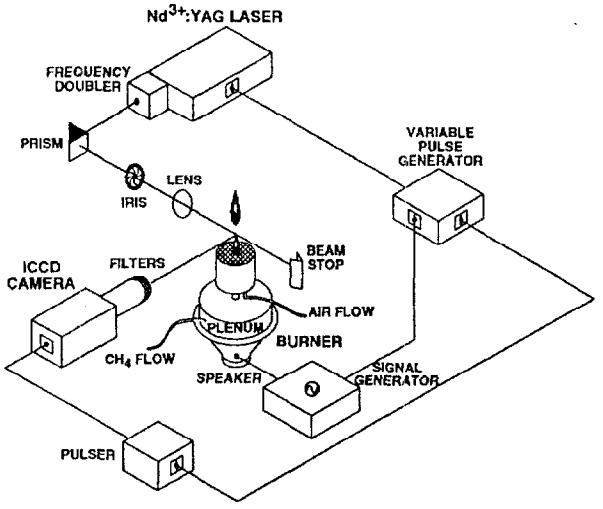

FIG. 1. The experimental configuration used for Rayleigh light scattering measurements of maximum temperatures in time-varying diffusion flames is shown.

the burner in the steady calibration flame were in excellent agreement with independent radiation-corrected thermocouple data obtained in an identical flame [14].

TFP has subsequently been used to map out MFT radial profiles as a function of height and phase for two different time-varying flames. The results of these mappings will be published elsewhere [15]. These temperature data have been used by Skaggs and Miller along with infrared diode absorption measurements to improve quantitative measurements of CO concentrations as a function of height and phase in the same flames [16]. During the full TFP mappings, two unusual behaviors were observed in the radial MFT profiles, namely, reduced maximum MFTs for certain flame phases at locations near the burner exit and apparently nonphysical localized variations of temperature for a limited number of phases and heights above the burner. The results presented here show that these behaviors are due to time-response limitations of TFP and soot deposition on the filament, respectively.

Experimental Approach

The experimental system for TFP measurements [6] and the burner [7] are described in detail elsewhere; only brief descriptions are provided here. The coannular burner consists of an 11-mm-diameter fuel tube ("UHP"-grade methane, 77.8 mm/s) surrounded by a 102-mm-diameter airflow (79.0 mm/s). The fuel tube is attached to a plenum containing a loudspeaker that is used to modulate the fuel velocity and thus lock the flame flicker frequency at 10 Hz. The entire burner is mounted on a vertical stage to position the flame relative to the β-SiC filament. The fuel-flow forcing is characterized by the peak-to-peak amplitude of the sine-wave voltage applied to the speaker. Two forcing conditions, moderate (0.75 V) and strong (1.5 V), were used.

The TFP experimental system is identical to that reported previously [6]. A 115-mm length of nominally 15-μm-diameter β-SiC fiber was stretched horizontally through the burner centerline, and emission from the fiber was imaged by a cooled CCD camera. A combination of the camera's electronic shutter and a mechanical chopper created an effective shutter time of 1.5 ms. Time-delay pulse generators triggered by a laser beam passing through the shutter opening provided triggers for the camera and the digital waveform generator used to apply the 10-Hz sine wave to the speaker. Radial TFP profiles were recorded for both flame-forcing conditions at heights ranging from 5 to 110 mm in steps of 5 mm. The TFP was calibrated, and MFTs were determined from the images as described previously [6].

The first step in the analysis of the line images is to integrate the intensity measured across the filament for each column of vertical pixels of the CCD camera and to subtract any background radiation. The integrated intensities are converted to temperatures on a pixel-by-pixel basis using a look-up table that relates the observed emission intensity to the measured filament temperature. This table is obtained by integrating the product of gray-body emission curves as a function of temperature and the spectral sensitivity curve for the silicon CCD array. A calibration point is necessary and is obtained by assigning the highest emission intensity observed along the fiber in the steady laminar flame at a height of 7 mm a temperature of 2000 K [14].

Rayleigh light scattering (RLS) measurements were also used to characterize temperature variations in regions of the time-varying flames where soot was not present. Figure 1 shows the experimental arrangement. The 100-mJ frequency-doubled output of a pulsed Nd^{+3}/YAG laser at 532 nm was used to induce Rayleigh scattering along the focused laser beam ($\approx$100 μm diameter). Scattered light was imaged and recorded by a gated (50 ns) intensified CCD camera to eliminate background flame emission. The laser was operated at 10 Hz and generated an electronic voltage pulse that provided central timing for the experiment.

Results

Variations of Maximum MFTs with Phase

Figure 2 shows two-dimensional images of the time-varying flames, recorded using a combination of OH laser-induced fluorescence and Mie scattering from soot, as a function of phase angle relative

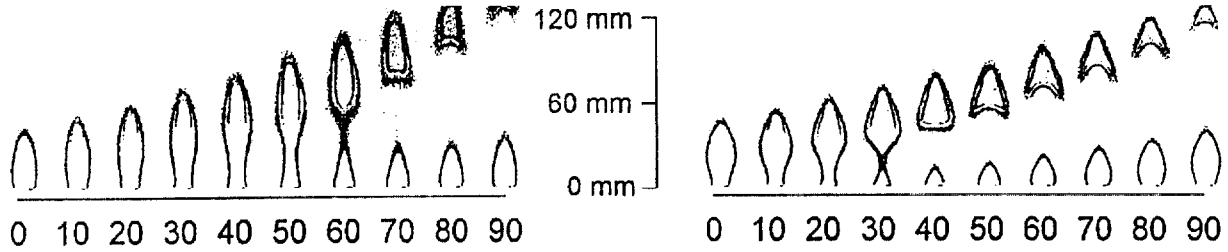

FIG. 2. Two-dimensional images of laser-induced OH fluorescence and soot Mie scattering are shown as a function of relative phase for moderately (left) and strongly (right) forced methane–air diffusion flames. The incident laser radiation at 283.55 nm excites the $Q_1(8)$ line of the $A^2\Sigma \leftarrow X^2\Pi_i$ (1,0) band of OH, and OH fluorescence and soot scattering are detected simultaneously [7,8]. The outer diffuse regions are due to OH, and the dark inner regions are due to soot.

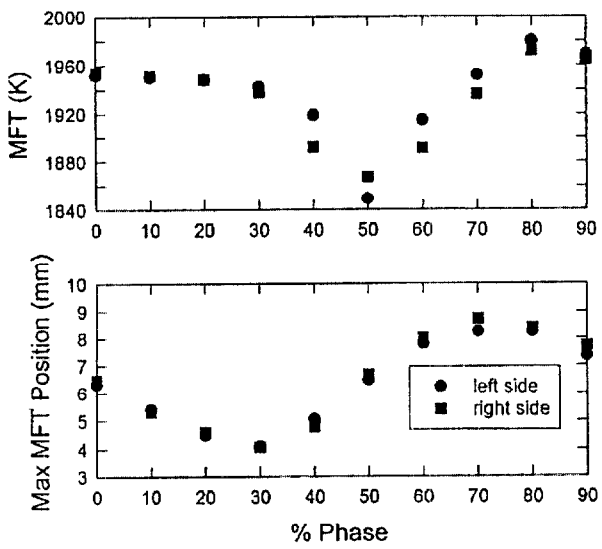

FIG. 3. Maximum MFTs and their radial locations are plotted as functions of relative phase angle for a time-varying methane–air diffusion flame with strong forcing (1.5 V). The filament is located 5 mm above the burner.

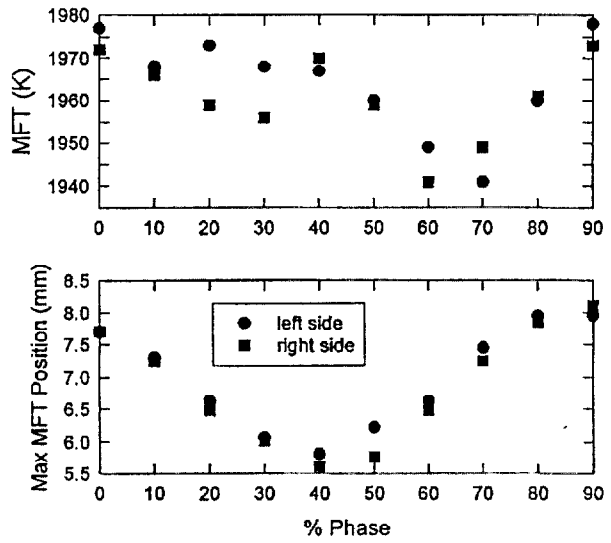

FIG. 4. Maximum MFTs and their radial locations are plotted as functions of relative phase angle for a time-varying methane–air diffusion flame with moderate forcing (0.75 V). The filament is located 5 mm above the burner.

to an arbitrary zero phase for both applied sine-wave voltages [8]. The images demonstrate the strong effects that acoustic forcing has on the flame shape and phase behavior. In the earlier MFT measurements for the 0.75-V time-varying diffusion flame, distinct variations in the maximum MFT and its location with phase were observed at 7 mm above the burner [6]. Figures 3 and 4 show similar results at heights of 5 mm above the burner for both the 1.5- and 0.75-V flames. Such variations were found for both flames at heights below the location of flame clip off (see Fig. 2). An important question is whether the MFT variations represent actual changes in flame temperature with phase or whether they are the result of an artifact of the TFP technique. RLS measurements are used to address this point.

RLS intensities along the laser beam were obtained by averaging 100 line images for a given flame phase. The measured RLS intensity, I_R, for a mixture of gases containing M species, can be written as [17]

$$I_R = KN \sum_{j=1}^{M} \sigma_j X_j \tag{1}$$

where K is a term that incorporates several experimental parameters including laser power, observation volume, lens collection efficiencies, and detector quantum yield; N is the total number of molecular species in the observation volume; σ_j is the RLS cross section for species j; and X_j is the mole fraction of species j. When the summation term in equation 1 is a constant, the RLS signal is directly proportional to the total number density in the observation volume and therefore inversely proportional to temperature. For this case, calibration of the RSL intensity for a known temperature allows varying temperatures to be determined.

For premixed combustion systems, the total RLS cross section is expected to vary little with the degree of reaction, and properly normalized RLS measurements can be used for accurate temperature determinations [18]. Unfortunately, the same is not true

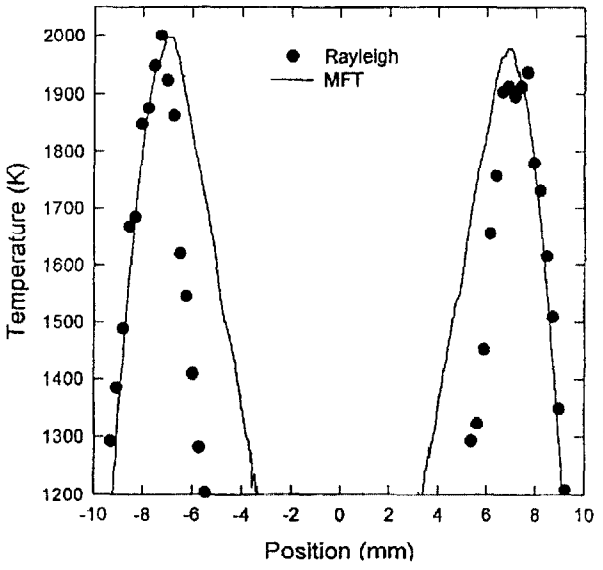

FIG. 5. Measured radial temperature profiles obtained using TFP and RLS are compared for the steady laminar methane–air diffusion flame at a height of 7 mm above the burner. Both approaches are calibrated assuming a maximum temperature of 2000 K, and the RLS-based measurements assume a constant total RLS cross section.

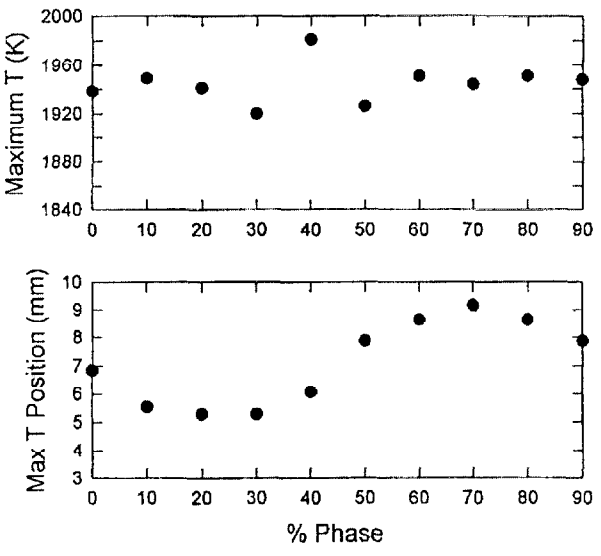

FIG. 6. Maximum temperatures measured 5 mm above the burner by Rayleigh light scattering and their radial locations as functions of relative phase angle are shown for a time-varying methane–air diffusion flame with strong forcing (1.50 V). The original data have been symmetrized to reduce noise.

for diffusion flames burning in air unless the unreacted fuel and air have the same RLS total cross sections. In general, the total RLS cross section will vary with mixture fraction. A constant total cross section only occurs when the fuel has been carefully chosen to match the RLS cross section for air [18]. Methane has an RLS cross section 2.34 times greater than air [17].

Kelman and Masri [19] have used computations of laminar counterflow methane–air diffusion flames to calculate the RLS intensity variation with mixture fraction. Their results show that assuming a constant RLS cross section (e.g., equal to σ_{air}) leads to large errors over much of the mixture fraction range. Fortunately, Kelman and Masri's calculations also indicate that the variation of the total RLS cross section is relatively mild over the mixture fraction range where the highest temperatures are expected and that even when the highest temperature measured by RLS assuming a constant total RLS cross section is subject to error, the maximum still occurs for the same mixture fraction as the true temperature. In fact, these calculations indicate that by calibrating the RLS signal using a known temperature in the high-temperature flame zone, it should be possible to accurately determine the highest flame temperature and its location. Because the primary interest is the behavior of the highest temperature region of the flame, the RLS intensity from room-temperature air was used as a reference and the minimum observed intensity at a height of 7 mm above the burner in the steady laminar flame was assumed to correspond to 2000 K, that is, the same assumption used to calibrate the TFP. This allows maximum flame temperatures and their positions along the radial direction to be obtained in the time-varying flames with the assumption of a constant total RLS cross section.

Based on Kelman and Masri's analysis, assuming a constant RLS cross section should lead to increasing errors on both the lean (overestimate) and rich (underestimate) sides of the highest temperature location. On the rich side, the error is expected to be several hundred degrees by the time the temperature has dropped to 1200 K. Figure 5 compares radial temperature profiles determined using both the TFP and RLS approaches for a height of 7 mm in the steady base flame. The results show the expected behaviors based on the foregoing discussion. The highest temperatures as well as their radial positions observed using calibrated RLS agree well with those using TFP. On the lean (outer) sides of the flame sheets, the two sets of measurements are in reasonable agreement, while on the rich (inner) sides, the RLS measurements fall well below the TFP temperatures. Based on Fig. 5, it is concluded that RLS can be used to record maximum flame temperatures and their locations in the time-varying flames.

Figure 6 shows maximum temperatures as determined from RLS measurements and their radial locations as a function of phase at a height of 5 mm for the 1.5-V flame. Comparison of Figs. 3 and 6 indicates that the locations of the temperature maximum and their magnitudes for MFTs and the RLS results agree well, except for those phases where the

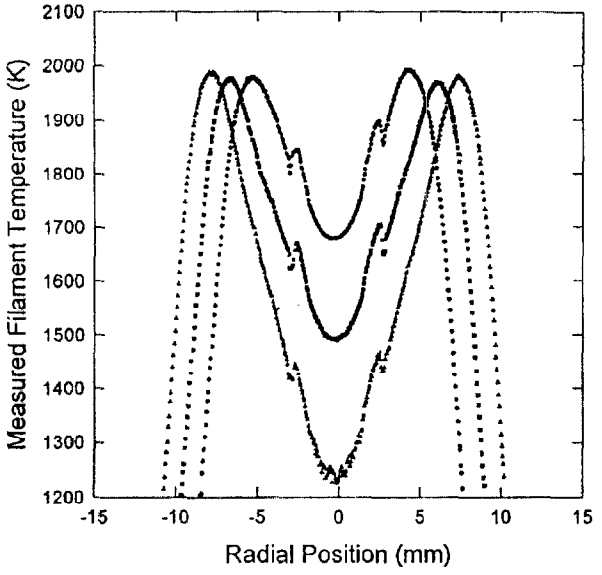

FIG. 7. Radial MFT profiles 20 mm above the burner for a moderately forced (0.75 V) flickering flame. MFTs from ≈1.0 to 2.7 mm from the centerline are perturbed by soot deposition. Phases shown: 80% (●), 90% (■), 0% (▲). See Fig. 2.

MFTs show a decrease. There is somewhat more scatter in the RLS data than for the TFP results, but it is clear that the RLS-based temperatures are constant within the experimental uncertainty (average peak temperature for the 10 phases is 1975 K, with an rms of ± 10 K). The sharp drops in temperature, ≈90 K for the 1.5-V flame (Fig. 3) and ≈25 K for the 0.75-V flame (Fig. 4), observed for certain phases in the TFP measurements are considerably larger than the uncertainty in the RLS measurements, thus indicating that the decreases are not real and must be an experimental artifact of the TFP technique.

Effects of Localized Soot Deposition

In the earlier TFP report, no effects of soot deposition on the filament were discussed (however, see reply to Professor Takahashi's question) in the time-varying flames, despite the fact that MFTs were measured at locations where soot volume fractions up to 1.8×10^{-6} existed [6]. This was not true for all of the current measurements. Figure 7 shows examples of MFT data where nonphysical MFT variations, that is, sharp discontinuities in the smooth profiles, are present. In severe cases, thickening of the emission image was observed, which is attributed to thermophoretic deposition of soot [20,21] on the filament.

Soot deposition effects for the flickering flames were only present for certain heights (10–25 mm for the 0.75-V flame; 10 mm for the 1.5-V flame) and radial positions at rich locations on the inside of the flame where the filament was never exposed to the highest flame temperatures. The radial positions of the MFT perturbations moved toward the flame center with increasing height for the 0.75-V flame. For both flames, the perturbations increased with the time that the filament remained at a given height above the burner. As can be seen in Fig. 7, the presence of soot deposition can result in either higher or lower MFTs (increases or decreases in measured intensity). Decreases in intensity were generally associated with small perturbations and short measurement times at a given height. As the soot was deposited for longer periods, higher MFTs than expected were observed, which grew with time.

Discussion

The results show that systematic errors can occur in TFP measurements in time-varying flames in addition to those due to disregard of radiation losses. The first of these is decreased MFTs with radial flame movements along the filament, which the RLS results indicate are not due to actual changes in the maximum flame temperature. Comparisons of the phases where the drops in maximum MFTs occur and the radial locations of the maxima indicate that the dips are primarily associated with the most rapid outward movements of the flame sheet and that the MFT perturbations increase with the rate of flame-sheet movement. These observations suggest that the reduced MFTs are the result of the finite time response of the TFP to a gas-temperature change.

As the flame sheet first approaches a given filament location, the local temperature begins to increase. If the inverse of the rate of temperature increase exceeds the filament response time constant, the rise in filament temperature will lag the true gas temperature. Once the region of maximum flame temperature passes, the filament begins to cool, and, if the steady-state MFT maximum has not been attained, the result is the observation of a lower maximum MFT. Note that the dip in temperature is larger for the 1.5-V case than for the 0.75-V case (compare Figs. 3 and 4) as expected because the 1.5-V flame moves over a wider radial extent, and the highest temperature flame region therefore passes over the filament at a higher speed.

An interesting result is that the largest effects are observed when the flame moves outward into air as opposed to inward flame movement. One reason for this is that the spatial temperature gradients on the air side of the flame are sharper, as can be seen in Fig. 5 of Ref. [6], and the temperature changes are faster as the flame moves outward with a given velocity. Furthermore, there is likely to be at least some preheating of the inside central regions of the flame so that temperature changes on the fuel side of the flame with inward movement are smaller. Another aspect that plays a role is the different molecular compositions on the two sides of the

high-temperature flame zone. Heat transfer to the filament depends on the thermal conductivity and kinematic viscosity of these gases. Both of these properties favor more efficient heat transfer and a shorter filament response time on the fuel side, thus allowing the filament to follow gas-temperature changes more rapidly.

Soot deposition on surfaces in a flame is expected to occur whenever soot is present. Perhaps it is surprising that TFP soot deposition effects are only observed for limited locations and phases. In our earlier work, the absence of soot deposition in soot-laden regions was attributed to soot being repeatedly deposited and burned off as the flame zone moved across the filament during each cycle. Soot deposition in the current experiments is observed only on the rich edges of the fluctuating flames when there is limited heating of the core region. For these cases, soot deposited during the brief periods when the rich flame edge is located closest to the centerline is never exposed to the high temperatures and reactive gases (i.e., OH radicals) necessary to oxidize the soot. As a result, soot continues to accumulate slowly at these positions. It is significant that soot deposition perturbations were found to continue to increase as long as a particular measurement height was studied.

The experimental results show that deposited soot can either increase or decrease the radiative emission from the filament. This observation is likely the result of competing effects. The measured β-SiC emissivity is 0.88 [1], which is somewhat lower than the value ($\approx$0.95) for soot [22]. Therefore, a thin layer of soot deposited on the filament is expected to increase the surface emissivity and hence the radiative heat loss from the filament surface. If the temperature of the filament remained constant, the emission intensity would increase. However, due to the increase in radiation, the temperature of the filament decreases due to the increased heat-loss rate. The strong temperature dependence for radiation means that the latter effect is likely to dominate, leading to lower emission intensities. Thus, for very thin layers of deposited soot, a drop in MFT should be observed. This effect should be particularly pronounced at high temperatures, where radiative heat-loss effects are high.

As soot continues to deposit on the filament over time, the surface area can grow significantly. A simple heat-transfer analysis that assumes a balance between convective and radiative heat transfer indicates that the radiative flux from the filament decreases with diameter with a dependence on diameter of one or less, with the dependence decreasing with increasing diameter. On the other hand, the total radiative emission per unit length is proportional to the available surface area and thus increases linearly with diameter. Therefore, as the diameter increases, one expects that the integrated radiation intensity per unit length ultimately increases, which will be interpreted as a higher MFT.

Both effects are evident in Fig. 7. Lower temperatures than expected are observed most clearly near the lean edges of the perturbations that are evident in the radial profiles. These regions correspond to regions of low soot volume fractions and slow soot deposition on the filament. Here the principal effect of soot deposition is to increase the filament emissivity and lower the MFT. Near the centers of the perturbed regions, the soot concentrations will be higher, and much higher deposition rates take place. At such locations, the local diameter of the fiber can increase significantly, leading to the observed rises in the MFT. Obviously, these effects are time dependent. For short total deposition times, one would expect to see decreases in MFTs at positions corresponding to high soot concentrations and very little effect in regions of lower soot concentration.

In a recent paper describing the use of thermophoretic deposition of soot onto a thermocouple for simultaneous measurement of temperature and soot volume fraction, McNeally et al. [23] have observed similar effects to those described here. When a thermocouple was rapidly inserted into a sooting location in hydrocarbon flames, the measured thermocouple temperature began to decrease after quickly attaining a maximum. Two distinct time behaviors were observed. The first was attributed to an increasing surface emissivity as the thermocouple was coated with a thin soot layer and the second to an increase in the effective diameter of the thermocouple as soot accumulated. It is interesting to note that these effects occurred over periods of seconds. Such times are consistent with the much longer periods observed in the current experiments because the flame movement substantially decreases the time available for soot deposition on the filament.

Final Comments

The effects of the finite time required for heat transfer to the β-SiC filament and soot deposition are certainly potential problems for interpreting TFP measurements. However, it must be kept in mind that the reason it is possible to observe these relatively small effects (on the order of 100 K or less) is the large signal-to-noise ratio available in the measurements. Highly precise, meaningful measurements are possible in the absence of these effects, and once they are better characterized, it should be possible to correct MFTs when they are present. It may also be possible to design experiments to minimize their influence. As an example, the time available for soot deposition can be limited by operating for a given flame condition for short time periods.

It is interesting to speculate how the high sensitivity of TFP along with the effects discussed here can be used for flame characterization. For instance, the decreases in MFTs with outward flame movement could be utilized to determine the filament time response under actual experimental conditions.

It should also be possible to make a variety of measurements concerning flame-generated soot. Variations in MFTs could be used to estimate the emissivity of deposited soot and to monitor deposition on and removal of soot from a filament. The latter measurement could provide detailed insights into the oxidation processes of in-flame soot.

REFERENCES

1. Vilimpoc, V., Goss, L. P., and Sarka, B., *Opt. Lett.* 13:93–95 (1988).
2. Vilimpoc, V. and Goss, L. P., in *Twenty-Second Symposium (International) on Combustion,* The Combustion Institute, Pittsburgh, 1988, pp. 1907–1914.
3. Goss, L. P., Vilimpoc, V., Sarka, B., and Lynn, W. F.,*J. Eng. Gas Tur. Power* 111:46–52 (1989).
4. Chen, T. H., Goss, L. P., Trump, D. D., Sarka, B., Vilimpoc, V., Post, M. E., and Roquemore, W. M., in *FED—Flow Visualization* (B. Khalighi, M. J. Braun, and C. J. Freitas, eds.), vol. 85, The American Society of Mechanical Engineers, New York, 1989, pp. 121–127.
5. Bédat, B., Giovannini, A., and Pauzin, S., *Expts. Fluids* 17:397–404 (1994).
6. Pitts, W. M., in *Twenty-Sixth Symposium (International) on Combustion,* The Combustion Institute, Pittsburgh, 1996, pp. 1171–1179.
7. Smyth, K. C., Harrington, J. E., Johnsson, E. L., and Pitts, W. M., *Combust. Flame* 95:229–239 (1993).
8. Shaddix, C. R., Harrington, J. E., and Smyth, K. C., *Combust. Flame* 99:723–732 (1994).
9. Kaplan, C. R., Shaddix, C. R., and Smyth, K. C.,*Combust. Flame* 106:392–405 (1996).
10. Shaddix, C. R. and Smyth, K. C., *Combust. Flame* 107:418–452 (1996).
11. Skaggs, R. R. and Miller, J. H., in *Twenty-Sixth Symposium (International) on Combustion,* The Combustion Institute, Pittsburgh, 1996, pp. 1181–1188.
12. Everest, D. A., Shaddix, C. R., and Smyth, K. C., in *Twenty-Sixth Symposium (International) on Combustion,* The Combustion Institute, Pittsburgh, 1996, pp. 1161–1169.
13. Smyth, K. C., Shaddix, C. R., and Everest, D. A.,*Combust. Flame* 111:185–207 (1997).
14. Richardson, T. F. and Santoro, R. J., personal communication, 1993.
15. Pitts, W. M., unpublished results.
16. Skaggs, R. R. and Miller, J. H., unpublished results.
17. Pitts, W. M. and Kashiwagi, T.,*J. Fluid Mech.* 141:391–429 (1984).
18. Dibble, R. W. and Hollenback, R. W., in *Eighteenth Symposium (International) on Combustion,* The Combustion Institute, Pittsburgh, 1981, pp. 1489–1499.
19. Kelman, J. B. and Masri, A. R., *Appl. Opt.* 33:3992–3999 (1994).
20. Eisner, A. D. and Rosner, D. E., *Combust. Flame* 61:153–166 (1985).
21. Rosner, D. E., *Transport Processes in Chemically Reacting Flow Systems,* Butterworths, Boston, 1986.
22. Siegel, R. and Howell, J. R., *Thermal Radiation Heat Transfer,* 3rd ed., Hemisphere, Washington, 1992.
23. McNeally, C. S., Köylü, Ü. Ö, Pfefferle, L. D., and Rosner, D. E., *Combust. Flame* 109:701–720 (1997).

COMMENTS

Larry Rahn, Sandia National Laboratories, USA. Can you tell us the size of the effect on your temperature calibration due to varying convective velocities?

Author's Reply. This question actually addresses the need to correct for radiative heat losses to the surroundings when TFP temperature measurements are recorded in high-temperature flame zones. We recognize the need for such corrections as emphasized by use of the "measured filament temperature (MFT)" to report results. The difference between the MFT and the surrounding gas temperature results from a balance between the convective heat transfer to the filament and the radiative losses. Estimation of these differences requires knowledge of a number of system parameters including probe diameter and surface emissivity and surrounding gas thermal conductivity, kinematic viscosity, and velocity. We have yet to attempt such corrections due to uncertainties associated with each of these properties as well as the appropriate expression to use to characterize the convective heat transfer. To minimize the need for such corrections, the TFP was calibrated at a single high temperature.

The velocity dependence results from variations in convective heat transfer from the hot gas to the filament. Varying velocities in the current experiments are due to the acceleration of the fluid by buoyancy forces arising from local heating due to combustion. Velocities are expected to increase from very low values near the burner exit to values on the order of 3 m/s near the flame tip [1]. The most rapid increase is near the burner exit, with velocities higher than 0.5 m/s being reached within 7 mm of the exit. The dependence of convective heat transfer on flow velocity is relatively weak and is expected to have an exponent between 0.4 and 0.5 [2], thus contributing a maximum potential variation of around 2.5 to the temperature correction for different positions covering much of the flame. The factor could be somewhat larger very near the burner exit.

REFERENCES

1. Santoro, R. J., Yeh, T. T., Horvath, J. J., and Semerjian, H. G., *Combust. Sci. Technol.* 53:89 (1987).
2. Pitts, W. M. and McCaffrey, B. J., *J. Fluid Mech.* 169:465 (1986).